*33rd EPS Conference on Plasma Phys. Rome, 19 - 23 June 2006 ECA Vol.**30I**, P-5.138 (2006)*

MSE Measurements of NTM Structure and Suppression With ECCD

C.C. Petty[1], R.J. Jayakumar[2], M.A. Makowski[2], D.P. Brennan[3], C.T. Holcomb[2], D.A. Humphreys[1], R.J. La Haye[1], T.C. luce[1], P.A. Politzer[1], R. Prater[1], M.R. Wade[1], and A.S. Welander[1]

[1]*General Atomics, P.O. Box 85608, San Diego, California 92186-5608, USA*
[2]*Lawrence Livermore National Laboratory, Livermore, California, USA*
[3]*Massachusetts Institute of Technology, Cambridge, Massachusetts, USA*

Abstract. Using direct analysis of the motional Stark effect (MSE) signals, an explicit measurement of the "missing" pressure-driven current density around the island location of a neoclassical tearing mode (NTM) is made for the first time. When the NTM is suppressed using electron cyclotron current drive, the measured changes in the current profile that restore the pressure-driven current are also found directly from the MSE measurements.

I. Introduction

Neoclassical tearing modes (NTMs) are magnetic islands that grow owing to a helical deficit in the bootstrap current density that is resonant with the spatial structure of the local magnetic field [1]. Although the theory of NTMs has been worked out in detail, experiments have yet to explicitly confirm the fundamental prediction of a local deficit in the bootstrap current density around the magnetic island location. The most interesting results published thus far were from JT-60U, where equilibrium reconstructions using motional Stark effect (MSE) measurements showed a localized decrease in the current density around the q=2 surface at $\rho \sim 0.2$ in the presence of a m/n=2/1 tearing mode [2]. Comparison of the equilibrium reconstructions with simulations led them to conclude that the bootstrap current density decreased within the island O-point [3]. In related experiments on JT-60U, the change in the plasma current enclosed between MSE channel locations around the q=1.5 surface was interpreted as being due to a decrease in the bootstrap current from a m/n=3/2 NTM [4].

The effect of NTMs on the (axisymmetric) current density profile has been examined on DIII-D using direct analysis of the MSE signals, yielding the first explicit measurement of the "missing" pressure-driven current density (Pfirsch-Schlüter and bootstrap) around the magnetic island location for both the m/n=3/2 NTM and m/n=2/1 NTM. The deficit in the pressure-driven current density disappears when electron cyclotron current drive (ECCD) is used to suppress the NTM by driving co-current at the resonant q surface. The magnitude and location of the ECCD are verified by the change in the current profile found directly from the MSE measurements.

II. Measurement of Missing Bootstrap Current

The bootstrap and Pfirsch-Schlüter currents are intrinsically related in neoclassical theory because the same forces drive these parallel currents. The Pfirsch-Schlüter current density can be experimentally determined from the MSE measurement of the vertical magnetic field [5] using the formula [6]

$$J_{PS} \approx J_{\phi} + \frac{1}{\mu_0 \hat{F}^2 \rho_b^2 R}\left(\frac{1}{\rho}\right)\frac{\partial}{\partial \rho}\left(\hat{F}\hat{G}\hat{H}\rho\frac{\partial R}{\partial \rho}RB_z\right) \quad . \qquad (1)$$

Here $\hat{F}$, $\hat{G}$, and $\hat{H}$ are dimensionless geometric parameters that can be calculated from an actual or model equilibrium, and J_ϕ can be ascertained from the B_z profile using Ampère's law [7]. The flux-surface-average bootstrap current density is related to the measured Pfirsch-Schlüter current density by [6]

$$\langle J_{BS}\rangle \approx J_{PS}\frac{R_0}{R\hat{F}}\left(1-\frac{R_0^2\hat{H}}{R^2\hat{F}}\right)^{-1}\frac{\eta}{\eta+1}\left[\frac{L_{31}}{\eta}+R_{pe}\left(L_{31}+L_{32}\right)+\left(1-R_{pe}\right)\left(1+\alpha\right)L_{31}\right] \quad . \quad (2)$$

Here $\eta = \partial \ln T/\partial \ln n$ and R_{pe} is the fraction of the total plasma pressure due to electrons; typical values for H-mode plasmas are η^{-1}=0 and R_{pe}=0.5. In the collisionless limit, the coefficients L_{31}, L_{32}, and α are functions only of Z_{eff} (very weakly) and the trapped particle fraction. For all the cases considered here, the magnetic island rotation frequency (10-30 kHz) is much faster than the MSE (no aliasing) bandwidth (1 kHz), so only the axisymmetric component of the current densities is determined.

The first explicit measurement of the spatiotemporal change in the bootstrap current density during the onset of a NTM is shown in Fig. 1. In this hybrid scenario [8] plasma on DIII-D, a m/n=3/2 NTM is destabilized by increasing β_N to 3.2 at 4250 ms. Electron cyclotron emission (ECE) fluctuations show the magnetic island to be centered at ρ=0.51, which is in good agreement with the location of the q=1.5 surface from equilibrium reconstruction using MSE data. Figure 1 shows that the onset of the m/n=3/2 NTM correlates with a growing deficit in $\langle J_{BS}\rangle$ measured nearby at ρ=0.54 (which lies between two MSE channels). At radii inside (ρ=0.35) and outside (ρ=0.74) the magnetic island, $\langle J_{BS}\rangle$ remains higher. In addition, a direct measurement of the safety factor minimum (around ρ=0.2) shows an abrupt increase from q_{min}<1 to q_{min}≈1.1 after the destabilization of the m/n=3/2 NTM. This is consistent with the disappearance of the sawtooth oscillation after 4700 ms.

The modification of the current density profile by various NTMs in these hybrid plasmas on DIII-D is shown in Fig. 2. For reference, the local J_ϕ and $\langle J_{BS}\rangle$ profiles before the onset of the n=1 or n=2 tearing modes are given (green). After the destabilization of a m/n=3/2 NTM (red), a small decrease in J_ϕ is observed around the plasma mid-radius; this is similar to the results reported in Ref. [4]. A direct analysis of the MSE signals clearly identifies this modification as being due to a ≈50% decrease in J_{PS} and $\langle J_{BS}\rangle$. Although the deficit in $\langle J_{BS}\rangle$ peaks within the magnetic island, its

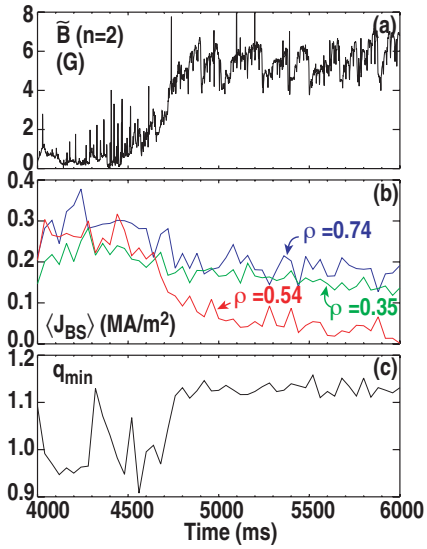

Fig. 1. Time history of (a) rms amplitude of n=2 mode, (b) bootstrap current density, and (c) safety factor minimum for hybrid plasma with β_N>3.1.

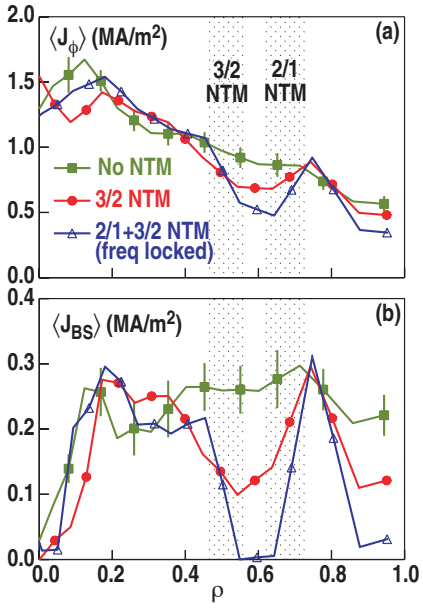

Fig. 2. Radial profile of (a) local toroidal current density, and (b) flux-surface-average bootstrap current density for hybrid plasmas with various NTMs. The radial extent of the islands, determined by ECE fluctuations, is shown.

radial extent is clearly wider than that of the island. A more dramatic case occurs when a m/n=2/1 NTM grows and frequency locks to a m/n=3/2 NTM (blue), resulting in a complete flattening of the pressure profile and a total loss of the pressure-driven current density between the two magnetic islands. Note that in numerically evaluating Eq. (1), the spatial derivatives are determined from linear interpolation (rather than spline interpolation) between the experimental B_z measurements. This gives a conservative account of the spatial resolution for the resulting current profiles.

III. ECCD Suppression of m/n=2/1 NTM

The first complete suppression of a m/n=2/1 NTM was obtained on DIII-D using co-ECCD at the q=2 surface [9]. Figure 3 shows a recent case from DIII-D with feedback control of the ECCD position to track changes in the q=2 location as beta is varied. Initially ECCD suppresses the m/n=2/1 NTM at β_N=2.3, which is followed by a ramp up of β_N to the no-wall stability limit ($\approx 4l_i$). This discharge is interesting from the standpoint of current profile analysis because the m/n=2/1 NTM reappears later in time at β_N=3.4 owing to an imperfect positioning of the ECCD (other discharges with slightly higher B_T sustained β_N above the $4l_i$ limit until the end of the gyrotron pulse [10]). The resulting spatiotemporal changes in the measured $\langle J_{BS} \rangle$ profile are plotted in Fig. 4. This color image shows the localized loss of bootstrap current density around the q=2 surface (ρ=0.63) during the initial m/n=2/1 NTM phase at low β_N; this deficit in $\langle J_{BS} \rangle$ disappears when ECCD suppresses the mode. As beta is ramped up from β_N=2.3 to β_N=3.4, the magnitude of $\langle J_{BS} \rangle$ is seen to increase until the onset of the m/n=2/1 NTM for the second time. The loss of bootstrap current is much more substantial for the high β_N phase, with a total loss of the pressure-driven currents observed between the m/n=3/2 and m/n=2/1 magnetic islands when these two modes frequency lock after 6340 ms.

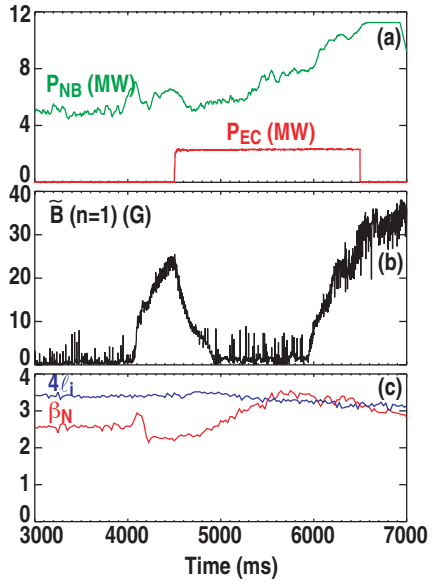

Fig. 3. Time history of (a) NBI and ECCD power, (b) rms amplitude of n=1 mode, and (c) normalized beta and no-wall stability limit. In addition to the m/n=2/1 NTM seen in (b), this hybrid scenario plasma also has a continuous and relatively benign m/n=3/2 NTM.

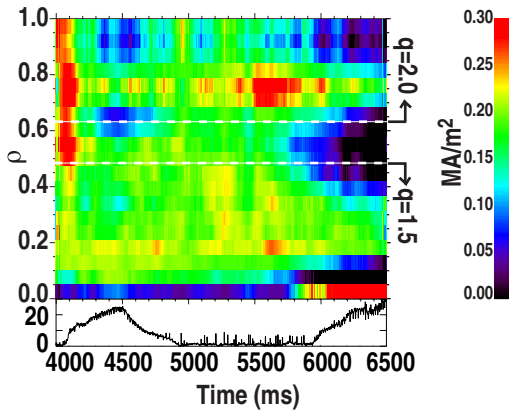

Fig. 4. Time history of (a) bootstrap current density as determined from Eq. (2), and (b) rms amplitude of n=1 mode for the discharge in Fig. 3.

When the m/n=2/1 NTM is suppressed using ECCD, the measured changes in the current profile that restore the missing bootstrap current at the q=2 surface are found directly from the MSE measurements. Figure 5(a) shows the measured $\langle J_{BS} \rangle$ profile before (green) and during (blue) the initial m/n=2/1 NTM phase at β_N=2.3 for the discharge in Fig. 3. A localized deficit in the bootstrap current density is observed after the onset of the m/n=2/1 NTM that peaks inside the magnetic island at q=2. As seen in Fig. 5(b), the ECCD utilized to suppress the

m/n=2/1 NTM is well positioned to replace this missing bootstrap current density. The EC current density is determined from the measured change in the total current density ($\langle J_{EC} \rangle \equiv \Delta \langle J_{||} \rangle$) shortly after the start of ECCD injection for a similar discharge without a m/n=2/1 NTM [the curves in (b) have been shifted by $\Delta\rho$=0.03 to compensate for a slightly different absorption location than in (a)]. The back EMF effect is not taken into account because determining the loop voltage profile requires longer time histories, which may explain the negative wings to the $\langle J_{EC} \rangle$ profile. The location and magnitude of the experimental $\langle J_{EC} \rangle$ are in good agreement with calculations using the TORAY-GA ray tracing code [11]. While the alignment between the ECCD and bootstrap current deficit is adequate for m/n=2/1 NTM suppression at β_N=2.3, the reappearance of the mode at β_N=3.4 is almost certainly due to the ECCD location being slightly further out than optimum.

IV. Conclusions

The change in the current density profile due to the onset and suppression of NTMs have been examined on DIII-D using direct analysis of the MSE signals. For plasmas with a rapidly rotating NTM, an axisymmetric analysis of the MSE data yields the first explicit measurement of the "missing" pressure-driven current density around the magnetic island location. The most dramatic case occurs when the m/n=3/2 tearing mode frequency locks to the m/n=2/1 tearing mode, resulting is a complete flattening of the pressure profile and a total loss of the Pfirsch-Schlüter and bootstrap current densities between the two islands. When the m/n=2/1 NTM is suppressed using ECCD, the measured change in the current density is well positioned to replace (and eventually restore) the bootstrap current deficit at the q=2 surface. Utilizing ECCD suppression of the m/n=2/1 NTM with feedback control of the current drive location, the β_N of hybrid scenario plasmas has been raised above the no-wall stability limit for the duration of the gyrotron pulse.

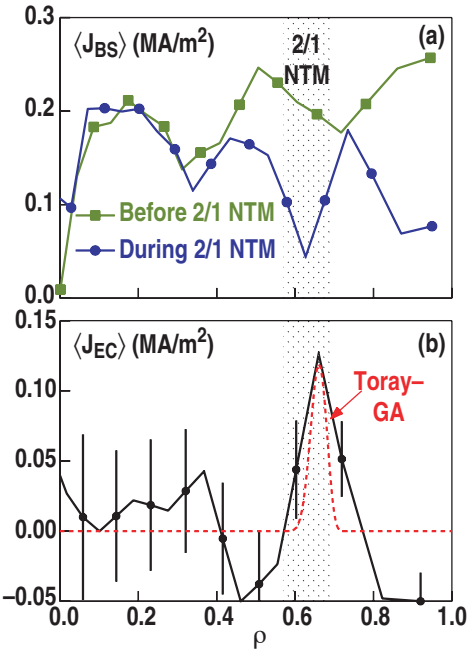

Fig. 5. Radial profile of (a) bootstrap current density, and (b) change in current density due to ECCD. The theoretical ECCD profile is also plotted.

This work was supported by the U.S. Department of Energy under DE-FC02-04ER54698 and W-7405-ENG-48.

References

[1] Z. Chang, *et al.*, Phys. Rev. Lett. **74**, 4663 (1995).
[2] T. Oikawa, *et al.*, Phys. Rev. Lett. **94**, 125003 (2005).
[3] T. Oikawa, *et al.*, Nucl. Fusion **45**, 1101 (2005).
[4] T. Suzuki, *et al.*, J. Plasma Fusion Res. **80**, 362 (2004).
[5] B.W. Rice, *et al.*, Phys. Rev. Lett. **79**, 2694 (1997).
[6] C.C. Petty, *et al.*, Plasma Phys. Control. Fusion **47**, 1077 (2005).
[7] C.C. Petty, *et al.*, Nucl. Fusion **42**, 1124 (2002).
[8] T C. Luce, *et al.*, Nucl. Fusion **41**, 1585 (2001).
[9] C.C. Petty, *et al.*, Nucl. Fusion **44**, 243 (2004).
[10] T C. Luce, *et al.*, J. Phys.: Conf. Series **25**, 252 (2005).
[11] K. Matsuda, IEEE Trans. Plasma Sci. **17**, 6 (1989).